Solid State Ionics 20 (1986) 111–124
North-Holland, Amsterdam

DISTRIBUTED CIRCUIT ELEMENTS IN IMPEDANCE SPECTROSCOPY: A UNIFIED TREATMENT OF CONDUCTIVE AND DIELECTRIC SYSTEMS

Robert L. HURT and J. Ross MACDONALD
Department of Physics and Astronomy, University of North Carolina, Chapel Hill, NC 27514, USA

Received 26 September 1985

Distributed elements have a long-established position in the field of impedance spectroscopy (IS). Presented here is a survey of a number of the more common elements, including the new distribution-of-activation-energies element. A unified treatment of the different IS levels (impedance, admittance, complex modulus, and complex dielectric constant) is proposed, enabling standard distributed elements to be used in the fitting of data taken from either conductive or dielectric materials. Various distributed elements are discussed and their responses are shown graphically and compared to one another in both 2-D complex plane projections and 3-D perspective plots.

1. Introduction

In the analysis of impedance spectroscopy (IS) data, such as impedance Z versus frequency ν, on solid or liquid electrolytes and dielectric materials, one does not usually have available a full mathematical expression for the impedance following from detailed microscopic analysis of all the physico-chemical processes occurring in the electrode/material system. Instead, one compares the data with the impedance of a plausible electrical equivalent circuit by some such means as complex nonlinear least squares (CNLS) fitting [1,2]. This equivalent circuit will be made up of circuit elements whose presence is related to physical processes which are believed likely to be present – such two-terminal elements as bulk and reaction resistances, double-layer space–charge capacitors, and Warbug diffusion impedances. In the present work, we summarize, discuss, and compare many of the non-ideal circuit elements, or frequency response functions, which are useful for fitting actual experimental small-signal frequency response data in this way.

Although we usually employ ideal resistors, capacitors and inductances in an equivalent circuit, actual real elements only approximate ideality over a limited frequency range. Thus an actual resistor always exhibits some capacitance and inductance as well and, in fact, acts somewhat like a transmission line, so that its output response to an electrical stimulus is always delayed compared to its input. All real elements are actually distributed because they extend over a finite region of space rather than being localized at a point. Nevertheless, for equivalent circuits which are not applied at very high frequencies (say over 10^7 or 10^8 Hz), it will usually be an adequate approximation to incorporate some ideal, lumped-constant resistors, capacitors and possibly, inductors.

But an electrolytic cell or dielectric test sample is always finite in extent, and its electrical response often exhibits two generic types of distributed response, either type requiring distributed elements in the equivalent circuit used to fit its IS data. The first type of response appears just because of the finite extent of the system, even when all system properties are homogeneous and space-invariant. Diffusion [3] can lead to a distributed circuit element of this type, the analog of a finite-length transmission line. When a circuit element is distributed, it is found that its impedance cannot be expressed as the combination of a finite number of ideal circuit elements, except possibly in certain limiting cases.

The second generic type of distributed response is quite different from the first, although it is also associated with finite extension in space. In all ordinary IS experiments, one uses electrodes of macroscopic

dimensions. Therefore the total macroscopic current flowing in response to an applied static potential difference is the sum of a very large number of microscopic current filaments originating and ending at the electrodes. If the electrodes are rough and/or the bulk properties of the material are inhomogeneous, the individual contributions to the total current will all be different, and the distribution in electrode surface and/or bulk properties will lead to an distributed conductance (many different elemental conductances) which will determine the total current.

The situation is even more complicated when small-signal frequency and time dependence is considered. Consider a material involving ion-hopping conduction. The immediate microscopic surroundings of different ions may be different at a given instant either because of inhomogeneous material properties or because the dynamic relaxation of the positions of atoms surrounding an ion has progressed a different amount for different ions [4]. The result may be described in terms of a distribution of relaxation times, which, for example, might be associated with a distribution of hopping barrier height activation energies. Such a distribution of relaxation times will lead to frequency-dependent effects which may, at least approximately, be described through the use of certain simple distributed circuit elements, such as the constant phase element (CPE) discussed later.

In this paper we describe various distributed circuit elements which have been or might be used in IS, show some of their little-known inter-relations, and discuss the important intensive and extensive properties of the elements considered. All elements discussed will be related, insofar as possible, to physical models. In order to aid in the recognition of the presence of distributed elements in experimental small-signal data, we shall show their full frequency responses by means of three-dimensional perspective plots [5]. There are four impedance-related quantities important in IS. These are all defined only in the small-signal linear regime and are impedance, $Z \equiv Z' + iZ''$; admittance, $Y \equiv Y' + iY''$; electric modulus, $M \equiv M' + iM''$, and complex dielectric constant $\epsilon \equiv \epsilon' - i\epsilon''$, where $i \equiv \sqrt{-1}$. Let C_c be defined as the capacitance of the empty measuring cell. Then these four complex quantities are inter-related as shown in table 1. Thus, for example, $Y \equiv Z^{-1} = (i\omega C_c)\epsilon$. The quantities ϵ and M are dimensionless while the units of Z and Y are ohms and siemens, respectively.

Table 1
Relations between the four basic immittance functions. Here $\mu \equiv i\omega C_c$.

	M	Z	Y	ϵ
M	M	μZ	μY^{-1}	ϵ^{-1}
Z	$\mu^{-1}M$	Z	Y^{-1}	$\mu^{-1}\epsilon^{-1}$
Y	μM^{-1}	Z^{-1}	Y	$\mu\epsilon$
ϵ	M^{-1}	$\mu^{-1}Z^{-1}$	$\mu^{-1}Y$	ϵ

Although circuit elements in equivalent circuits involve quantities whose magnitudes depend on electrode area, we shall, for simplicity, give all formulas and definitions herein in unit area terms and will use the same symbols for all such quantities as admittance and admittance per unit area. Although Z, Y, or $C_c\epsilon$ may be measured directly, it is often valuable to examine 3-D plots not just of the data in their original form but also such plots of several or all of the other three related quantities. Further, the distributed elements we consider all show their simplest 3-D behavior when plotted in a particular one of the four types of 3-D plots mentioned above. This effect is illustrated for the ZC element (see below).

The next section deals with two intrinsically different types of electrical response, that of dielectric and of conductive systems. General system immittance functions are defined which include both types of response and allow generalizations and simplifications of the succeeding work. In particular, they permit one to use a single function which readily yields all the eight M, Z, Y and ϵ response functions for unified dielectric and conductive systems. The following sections first deal with general and specific homogeneous diffusion situations and then with the constant phase element (CPE), which may be related to inhomogeneous diffusion. Then various composite elements which involve the CPE explicitly or implicitly are discussed, and the work concludes with discussion of distributed elements which are associated with a distribution of relaxation times (DRT) or activation energies (DAE).

2. Conductive, dielectric and unified response

Let us define a Conductive System as one which

exhibits non-zero dc conductance, while a Dielectric System may be defined as one without dc conductance. These are taken to be intrinsic properties of the material of interest and are not associated with blocking at electrodes, etc. Thus a dielectric material with a resistor in parallel with its arising, for example, from surface conduction, is not a conductive system under the present definition, nor is a conductive system with a capacitor in series with it a dielectric system. We shall distinguish between dielectric system and conductive system quantities by a subscript D or C. We shall show that because of a duality between the two kinds of systems, elements used in the dielectric area may also be simply adapted and used as well for conductive systems.

We may illustrate the difference between a D and a C system by DRT examples. Consider first a D-system with a continuous DRT, one whose relaxation time probability density is $\mathcal{G}_D(\tau)$, where τ is a relaxation time. The system response may be considered to be made up of an infinite number of composite differential circuit elements in parallel, each such element consisting of an elemental resistor and capacitor in series. Alternatively, a C-system involving a continuous DRT, $\mathcal{G}_C(\tau)$, may be considered to involve an infinite number of elemental parallel R–C units in series [6]. Unless one or more capacitances in the first system is infinite or one or more resistances in the second system is infinite, the first will pass no direct current and the second may do so.

We may now write the complex dielectric constant ϵ_D of the D-system and the impedance Z_C of the C-system [6] as

$$\epsilon_D = \epsilon_\infty + (\epsilon_0 - \epsilon_\infty) \int_0^\infty \frac{\mathcal{G}_D(\tau)\,d\tau}{1 + i\omega\tau} \tag{1}$$

and

$$Z_C = R_\infty + (R_0 - R_\infty) \int_0^\infty \frac{\mathcal{G}_C(\tau)\,d\tau}{1 + i\omega\tau} \quad . \tag{2}$$

Results may be slightly more complex when a DAE is present [7]. The normalization implicit in $\mathcal{G}_D(\tau)$ and $\mathcal{G}_C(\tau)$ is taken such that when $\omega \to 0$, $\epsilon_D \to \epsilon_0$ and $Z_C \to R_0$. Note that when $\mathcal{G}(\tau) = \delta(\tau - \tau_0)$, where δ is a Dirac delta function, these results yield just simple Debye response, response with a single, non-distributed relaxation time. Here we have introduced the new quantities, ϵ_0 and R_0, and the corresponding $\omega \to \infty$ ones, ϵ_∞ and R_∞. It will be convenient and is indeed customary for one to deal with ϵ_D and Z_C quantities whose real parts are normalized to unity at $\omega = 0$. We shall denote such normalization, where appropriate, with a subscript N. Then we may write

$$\kappa_D \equiv \kappa_{DN} \equiv I_D \equiv \left(\frac{\epsilon_D - \epsilon_\infty}{\epsilon_0 - \epsilon_\infty}\right) = \int_0^\infty \frac{\mathcal{G}_D(\tau)\,d\tau}{1 + i\omega\tau} \tag{3}$$

and

$$Z_{CN} \equiv I_C \equiv \left(\frac{Z_C - R_\infty}{R_0 - R_\infty}\right) = \int_0^\infty \frac{\mathcal{G}_C(\tau)\,d\tau}{1 + i\omega\tau} \quad . \tag{4}$$

We can deal with complex capacitances instead of complex dielectric constants, if desired, by writing $C_D \equiv C_c\epsilon_D$, $C_\infty \equiv C_c\epsilon_\infty$, etc. Note that we have introduced in eqs. (3) and (4) the unified, normalized immittance function I_i which is a normalized complex dielectric constant function when i = D or a normalized impedance when i = C.

Now come some interesting and useful results. Suppose that for any reason we find that I_D and I_C are identical functions of frequency. In the present example this would require that the D-system $\mathcal{G}_D(\tau)$ function be identical in form with the C-system $\mathcal{G}_C(\tau)$ function. If $I_D = I_C$, this equality induces a correlation or unification between the corresponding D and C systems. Thus whenever an I_C or I_D function is specified, duality between systems leads to an implicit or explicit specification of a model for the other system. The connections which follow for various immittance function levels for the two separate systems are shown

Table 2
Relations between normalized immittance functions for various systems when $I_D = I_C$.

Dielectric	Conductive	Unified
Y_{DN} ⟷	M_{CN} ⟷	$L_{iN} \equiv L_i = \mu I_i$
κ_{DN} ⟺	Z_{CN} ⟺	$I_{iN} \equiv I_i$
M_{DN} ⟷	Y_{CN} ⟷	$S_{iN} \equiv S_i = I_i^{-1}$
Z_{DM} ⟷	κ_{CN} ⟷	$T_{iN} \equiv T_i = (\mu I_i)^{-1}$

in table 2, where the two double-ended arrows together are used to emphasize the primacy of the $Z_{CN} = K_{DN}$ equality. All the other double-ended arrows indicate equalities which follow because of the table 1 relations between the other normalized D and C system immittance functions. For normalized functions such as we shall discuss later, it is convenient to replace $\mu = i\omega C_c$ by $\mu = is$, where s is a normalized frequency variable. We shall do so in the following: We have selected new symbols, as shown in the last column of the table, to designate the unified-system normalized immittance functions and will generally omit the N subscript for these functions. We see that $L_D = Y_{DN}$ and $L_C = M_{CN}$, for example, and that knowledge of I_i and μ alone is sufficient to allow all the eight D and C system normalized immittances to be readily obtained.

These results show that we need only to consider the various distributed element functions which may be of use in IS data analysis at the I_i level; specific D and C system response results follow automatically. Although the L_i, S_i and T_i functions are simply related to I_i as we have seen, rather than present just I_i response, it is worthwhile to examine L_i and S_i as well, particularly using 3-D perspective plots. The T_i function is less interesting for most materials and will not be considered in as much detail as the others.

3. Specific response functions

3.1. Diffusion

The first distributed element introduced into electrochemistry was the infinite-length Warburg impedance [8], which models the one-dimensional diffusion of a particle in a homogeneous right half-space. This response is also completely analogous to wave transmission on a uniform semi-infinite RC transmission line [3]. But experimental cells are never infinite in extent nor are real transmission lines. Thus one needs diffusion response for a finite-length region, say that between two identical, plane parallel electrodes a finite distance apart. Such response, that of the finite-length Warburg, FLW, has been employed in liquid and solid electrolyte work for a long time [9,10] and differs from that of the infinite length Warburg only at low frequencies. General FLW response is analogous to that of a finite-length transmission line, shorted for a C-system and open-circuited for a D-system [3,7,11].

An expression for I_i FLW response is given in table 3. There the normalized frequency variable s is $\ell_e^2(\omega/D)$, where ℓ_e is the effective length over which diffusion occurs and D is the diffusion coefficient of the diffusing particle. Note that when $s \gtrsim 3$, the value of the tanh term is essentially unity and FLW response reduces to that for the infinite length Warburg. Such response is intensive, independent of sample dimensions when, e.g., admittance rather than admittance per unit area is considered. Alternatively, when $s \to 0$, FLW response is extensive and depends on the distance between the electrodes. The C-system impedance for FLW response is just

$$Z_{CFLW} = R_\infty + (R_0 - R_\infty) I_{CFLW}\,, \tag{5}$$

and the corresponding complex dielectric response is

$$\epsilon_{DFLW} = \epsilon_\infty + (\epsilon_0 - \epsilon_\infty) I_{DFLW}\,, \tag{6}$$

Table 3
$I_i(s, \psi_i)$ expressions for various distributed elements.

No.	Physical process/name	Acronym	I_i formula
1	uniform diffusion	FLW	$\tanh(\sqrt{is})/\sqrt{is}$
2	nonuniform diffusion?	GFW	$\tanh(is)^{\psi i}/(is)^{\psi i}$
3	constant phase element	CPE	$(is)^{-\psi i}$
4	distribution of relaxation times	ZC	$[1 + (is)^{\psi i}]^{-1}$
5	distribution of relaxation times	DC	$[1 + is]^{-\psi i}$
6	Williams–Watts response	WW	I_{iWW}
7	distribution of activation energies	DAE	I_{iDAE}

where I_i is, as usual, either I_C or I_D. We shall show graphs of FLW and other response later.

The second item in table 3, also related to diffusion, is an expression for a type of generalized finite length Warburg response [7], GFW. Its equation differs from that of FLW only by the replacement of the 0.5 exponent in the FLW expression by ψ_i, with $0 < \psi_i < 1$. Although one could take $\psi_C = \psi_D = \psi$, it has become customary in the principal case where the same formula has been used previously for both C and D response (see later discussion of ZC response) to set $\psi_C = 1 - \psi_D$. Then the GFW L_i and S_i functions both involve $(is)^n$ response in the frequency region where finite length effects may be neglected. For example if $I_i = (is)^{-\psi_i}$, then $L_D = Y_{DN} = isI_D = (is)^{1-\psi_D}$ and $S_C = Y_{CN} = I_C^{-1} = (is)^{\psi_C}$. Therefore $n = \psi_C = 1 - \psi_D$, and the admittance calculated for either a D- or a C-system exhibits the same frequency dependence. Note that for the FLW function, where $\psi_i = 0.5$, it does not matter whether one takes $\psi_D = \psi_C = 0.5$ or $\psi_D = 0.5 = 1 - \psi_C$. Various distributed elements included in the term, "universal dielectric response", by Jonscher are discussed below (the CPE) or elsewhere [7].

3.2. Constant phase element

The above considerations lead naturally to the CPE function introduced by Fricke [12] and Cole and Cole [13] and discussed recently in some detail [14]. Item three of table 3 shows that the CPE, which is defined for all frequencies, is the infinite-length diffusion limit of the FLW when $\psi_i = 0.5$ or the arbitrary-ψ_i infinite-length limit of the GFW. Now Schrama [15] has shown that the CPE with $0 < \psi_i < 1$ may be interpreted as representing homogeneous diffusion for $\psi_i = 0.5$ or inhomogeneous diffusion for other ψ_i values, a mathematical analog of wave propagation along a non-uniform continuously distributed semi-infinite transmission line. It was this result which led to the GFW and its tentative identification as a heuristic, approximate formula for non-uniform one-dimensional diffusion in a finite region. It is proposed as a temporary expedient until a detailed theory of such response becomes available.

Thus one model for the CPE is that of semi-infinite non-uniform diffusion. Another is its interpretation as a DRT [6]. But the DRT function associated with the CPE is non-normalizable, another indication that the CPE is only valid over a limited frequency range. In any physically realistic model there should be both a shortest and a longest relaxation time; the CPE exhibits neither. Let us consider the FLW, a model whose response reduces to that of a single series RC circuit as $s \to 0$ for the D-system and to a parallel RC circuit for the C-system. Thus, its modification of the CPE is physically reasonable for $s \to 0$. Further, in this limit the response is no longer intensive but becomes extensive. But there remains a problem as $s \to \infty$. The CPE, the GFW and the FLW all yield a non-physical infinite conductance (when $\psi_i \neq 1$) when $s \to \infty$. Now the diffusion length associated with one-dimensional diffusion is $\ell_{D\ell} = \sqrt{D/\omega}$, which goes to zero as ω or s goes to infinity. But it is obvious that ordinary diffusion theory, which involves a continuum, average process, will not apply when the diffusion length becomes comparable to the mean free path length of the diffusing elements. Thus the CPE, which suffers from both a $s \to 0$ and a $s \to \infty$ catastrophe must be modified at both ends of the frequency spectrum in order to represent a physically reasonable response model.

Although we have presented the CPE in table 3 at the I_i level for comparison with the other response functions listed, it cannot be converted to the Z or ϵ level by means of eqs. (5) or (6) since the equivalent R_0 or ϵ_0 quantities are infinite. Instead we must just consider the present I_{iCPE} as a normalized, dimensionless form of the CPE which, in general, may be written as [14]

$$Z_{CCPE} = Y_{CCPE}^{-1} = [A_{0C}(i\omega)^{\psi_C}]^{-1}, \tag{7}$$

or

$$\epsilon_{DCPE} = M_{DCPE}^{-1} = [A_{0D}(i\omega)^{\psi_D}]^{-1}. \tag{8}$$

Depending on the choice of A_{0i}, general CPE response can be either intensive or extensive. Again, it should be emphasized that eqs. (7) and (8) should only be applied for the range $0 < \omega < \infty$ to insure physical realizability.

3.3. Two DRT distributed elements

Two empirical distributed elements long used in the dielectric system area are those of Cole and Cole [13], and Davidson and Cole [16] (the DC element). As shown in table 3 in rows 4 and 5 at the I_i level, they may be associated with specific distributions of

relaxation times. The Cole–Cole dielectric response function has also been proposed as a conductive system distributed element [17] and has proved very useful in fitting IS data for many different conductive systems [7,17,18]. Since I_{CZC} leads to a curve in the conjugate impedance plane which is an arc of a circle whose center falls below the real axis (for $0 < \psi_C < 1$), it has been termed the ZARC function [18]. Note that it is symmetric about its center point. Exactly the same shape (an ϵARC) occurs, of course, when I_{DZC} is plotted in the complex dielectric constant plane (a Cole–Cole plot). Because of its impedance-plane shape and its original introduction by Cole and Cole [13], it seems reasonable to designate the general I_{iZC} function by the ZC acronym.

It is interesting to note that the I_{iZC} function may either be considered as a unified distributed element in its own right or as a composite element, a combination of an ideal circuit element and a CPE. For example, ZARC response and I_{CZC} are obtained from a resistor, $(R_0 - R_\infty)$ in parallel with a CPE, and ϵARC response and I_{DZC} are obtained from the series combination of a capacitor, $(C_0 - C_\infty)$ and a CPE [18]. One may also define the YARC and MARC functions, ones which lead to a displaced semicircle in the admittance plane and in the complex modulus plane, respectively. The former may be synthesized by means of a resistor in series with a CPE and the latter by means of a capacitor in parallel with a CPE.

Unlike the ZC, the DC element leads to an asymmetric curve in the complex plane, one with a peak toward the low frequency side of the curve. Of course the DC element involves a different DRT than does the ZC. Neither element is consistent with a temperature independent DAE [19], yet the presence of a DAE (leading to an associated DRT) is probably more common experimentally than that of a DRT unassociated with a DAE. Although the ZC and DC elements may fit dielectric or conductive system data very well, it is inconsistent to use them for fitting when it is found that the system is thermally activated with a temperature independent DAE. Unfortunately, this fact has not been well appreciated in the past and they have indeed been often used in thermally activated situations where such a DAE is likely to be present.

Finally, it should be mentioned that neither the ZC nor the DC leads to physically reasonable response at both frequency extremes. The requirement that a realizable system should have a largest (non-infinite) and a smallest (non-zero) relaxation time leads to I'' response proportional to s in the limit of low frequencies and to s^{-1} in the high frequency limit. This matter often seems to be of no practical consequence, however, since measurements frequently are not (or cannot conveniently be) extended to the extreme frequency regions where such response must occur. Nevertheless, it is another reason why more physically realistic distributed elements than the ZC and DC should be used, when practical, in IS fitting and data interpretation.

3.4. The Williams–Watts and DAE distributed elements

Long ago, Kohlrausch [20] proposed the stretched exponential as an empirical relaxation function in the time domain,

$$q(t) = q(0) \exp[-(t/\tau_0)^{\psi}] \,. \tag{9}$$

In the case of dielectric relaxation, $q(t)$ may represent total charge or polarization and τ_0 a relaxation time, a single Debye time constant when $\psi = 1$. In more recent times the frequency domain response following from eq. (9) has been discussed by Williams and Watts and used for fitting of dielectric system response data [21]. Since then, such Williams–Watts (WW) response has been found to follow from several different theoretical models, and WW transient and frequency response functions have been used to fit a variety of relaxation data for dielectric, conductive, and mechanical systems (see ref. [22] for many theoretical and experimental references). Incidentally, WW response leads to an asymmetric curve, rather like that of the DC, when I_{iWW} is plotted in the complex plane.

Unfortunately, it is not possible to obtain a simple exact expression for I_{iWW}. Thus the WW fitting that has been carried out so far has not been a definitive test of the appropriateness of WW frequency response for the various experimental data sets used. Further, only the imaginary part of the response has generally been compared with approximate WW frequency response predictions. A more appropriate approach is to use CNLS fitting of both the real and imaginary parts simultaneously. Although this has been impractical previously for WW frequency response fitting, a new, relatively simple, complete complex expression for WW frequency domain response has recently

been developed [23]. It may be used for either dielectric or conductive system data fitting. This expression is approximate but is nevertheless very accurate for $0.2 \leqslant \psi \leqslant 1$. It has been incorporated as part of an extensive and flexible CNLS fitting routine available from one of us (J.R.M.). This computer program allows none, one, or many distributed elements of different types to be made a part of an equivalent circuit also involving ideal circuit elements connected in different ways. Note that all fitting circuits must involve the geometrical capacitance C_∞ already introduced above, although sometimes the measurement frequency range does not extend high enough for this element to have an appreciable effect on the measured response. It always bridges the two electrodes of a measuring cell.

The DAE distributed element of table 3, line 7 also cannot be expressed exactly in simple closed form in the most general case. But it can be represented by an integral which can be easily evaluated numerically and has been incorporated as a part of the CNLS fitting program mentioned above. There are several forms of the DAE but they all involve an activation energy probability density which depends exponentially on the activation energy (properly, enthalpy of activation). The transient response of the general DAE model was discussed in detail some time ago [24] and the corresponding frequency response, that of I_{iDAE}, has only recently been considered [7]. It should be noted that although all of the distributed elements considered herein show power-law frequency response of the CPE type, at least over limited frequency ranges, only the DAE also exhibits physically realizable response in both frequency extremes.

The most general form of the DAE (which should properly be designated the EDAE, for exponential distribution of activation energies) involves two slope parameters, ϕ_{i1} and ϕ_{i2}, which are related to frequency-response power-law exponents, such as the ψ_i's already introduced. But unlike the ψ_i's, which must fall in the range [0,1], the ϕ_i's may take on values between $-\infty$ and $+\infty$. Nevertheless, when they are reasonably close to 0.5, they play a role like the ψ_i's. There are two simplified forms of the general DAE where only a single ϕ_i occurs, the DAE_1 and the DAE_2. For the DAE_1, which leads to an asymmetrical complex plane shape like that of the DC or WW, one has $\phi_{i1} = \phi_{i2} = \phi_i$. On the other hand, when $\phi_{i1} = -\phi_{i2} = \phi_i$, one has the DAE_2, a model which leads to a symmetric shape in the complex plane like that of the ZC. When neither of these conditions applies, one has the general DAE, a model which can lead to even more complicated shapes in the complex plane [7]. Finally, there is one other parameter present in the DAE model which needs to be mentioned; r (or r_2), the ratio of maximum to minimum relaxation times present in the system. It can become very large at low temperatures.

Now it is found that when "data" covering a finite frequency range and derived from one of the distributed element models of rows 1 through 6 of table 3 is fitted with the DAE model using full CNLS, an exceptionally good fit is found [7,22,25]. Thus one or another form of the DAE can simulate any of the other distributed elements considered herein over the frequency range of experimental interest. We have already mentioned that the DAE is physically reasonable in the frequency extremes while the other distributed elements are not. Another important virtue of the DAE model is that it leads to explicit temperature dependence predictions for the ϕ_i's of the model, predictions which usually seem to be in good agreement with experimental results. On the other hand, no specific temperature dependence predictions are available for the ψ_i's of the other distributed elements, and they are inconsistent with a temperature independent distribution of activation energies.

4. Graphic illustration of response curves

The first element to be considered will be the CPE. We shall suppress the i subscript of ψ_i and ϕ_i in this section for simplicity. Only the response of the DAE_1 model will be considered here since that of the other DAE models has been discussed elsewhere [7]. The CPE must be treated by itself since, as noted previously, it is the only element which does not have a convergent value for both low and high frequencies in any system. The CPE thus cannot meaningfully be included in perspective 3-D plots with any of the other elements. Fig. 1 shows I^* and S plots (corresponding to Z^* and Y in a conductive system) for a CPE with an exponent of 1/2. It is easy to see how this element derives its name from the constant phase angle in the complex plane projection. The angle, measured from the real

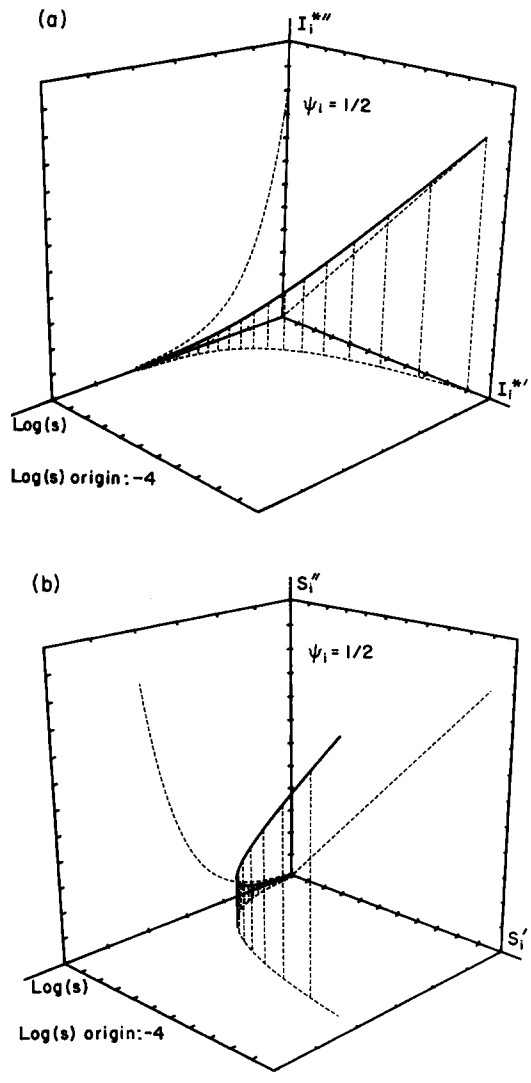

Fig. 1. 3-D perspective plots of the constant phase element (a) in the I^* plane (corresponding to impedance or dielectric response) and (b) in the S plane (corresponding to admittance or complex modulus). The normalized $\log_{10}$ frequency axis is marked in units of 1 and in (a) the I axes are in units of 7.1 while in (b) the S axes are in units of 0.067.

axis, is simply $\theta \equiv \pi\psi_i/2 = \pi/4$. The phase angle for the S plot is the same here. Notice the great difference in frequency dependence between the I^* and S curves, however.

Next to be considered are the ZARC–Cole, or ZC element, and the YARC distributed element. The complex plane admittance plot of a YARC has the same form as the complex plane impedance plot of a ZC, hence its name. The responses of these two elements are illustrated in fig. 2 in each of the four different systems. It turns out that the best way to directly compare these two elements on the same graph is to display them in different systems, with one system being the complex conjugate of the reciprocal of the other. For instance, fig. 2a presents an I^* plot for the ZC (corresponding, for example, to Z^*) and an S plot for the YARC (corresponding to Y). We shall not generally distinguish between an I and an I^* plot when the context is clear. Fig. 2a also exhibits an important aspect of the response of the ZARC and YARC elements: there are converged limits at both the low and high frequency ends and there is a clear peak in the imaginary values (centered at $s = 1$ for these normalized data). In fact, of all the distributed elements discussed in this section, only the YARC exhibits this peaked behavior in the S system – for the others it is found in the I^* system, as with the ZC. Note particularly that the shapes of the I^* and S projection curves are identical (but with opposite frequency dependence) for the Im–log(s) and Im–Re planes.

Concentrating only on the ZC response curves, one sees in fig. 2b that for low frequencies the imaginary component of T^* (corresponding to κ^*) is about 100 times greater in magnitude than the real component. Note that because of this extreme variation, a log–log plot is presented for these T and L systems. At high frequencies, the two are of approximately the same order of magnitude. The S and L plots (figs. 2c and 2d) appear to be nearly identical, and indeed they are very close. However, while L approaches zero at high frequencies, S approaches one. The great similarity between these graphs also comes from the symmetries introduced by considering only $\psi = 1/2$. Figs. 2e and 2f show the same two curves for $\psi = 1/3$, where these symmetries have broken down.

The general trends exhibited by the ZC element in these four systems are shared by all of the other distributed elements to be covered in this section. It is somewhat difficult to easily see the differences between elements when viewed in systems other than I^* since it is the only one which is well behaved and converged for both ends of the frequency spectrum. So for easier reference, all major comparisons between elements will be made using I^* plots.

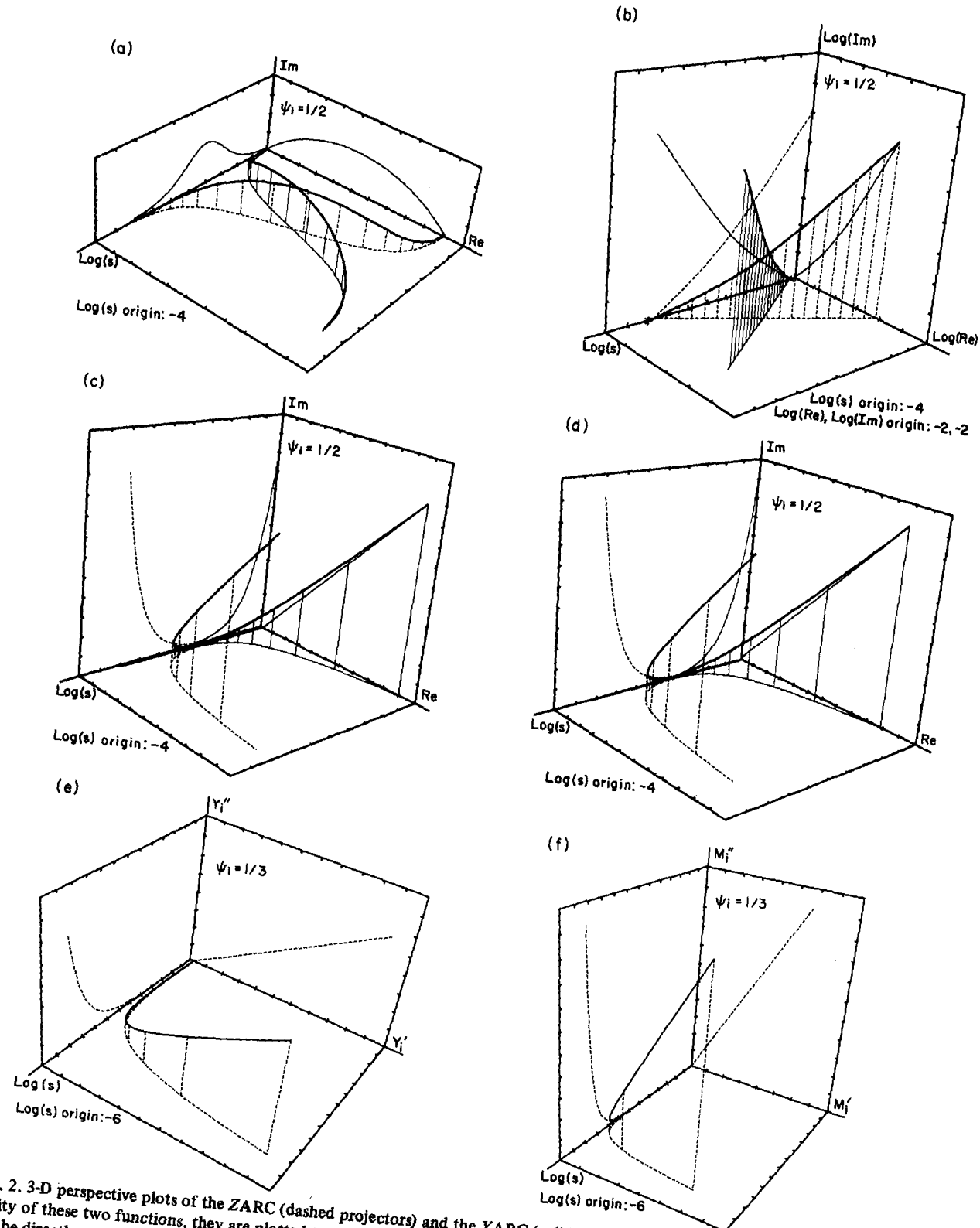

Fig. 2. 3-D perspective plots of the *ZARC* (dashed projectors) and the *YARC* (solid projectors). Because of the mathematical similarity of these two functions, they are plotted together in different systems to bring out these symmetries even though they cannot be directly compared. The units of log(*s*) are 1. For the first four plots, the corresponding *ZARC*/*YARC* systems plotted are: (a) *I*/*S*, Re/Im units = 0.1; (b) log(*T*)/log(*L*), log(Re)/log(Im) units = 1; (c) *S*/*I*, Re/Im units = 7.2; (d) *L*/*T*, Re/Im units = 7.1. Plots (e) and (f) show admittance and modulus plots for a *ZARC* with $\psi = 1/3$. For (e) the *Y* units are 4.8 and for (f) the *M* units are 250.

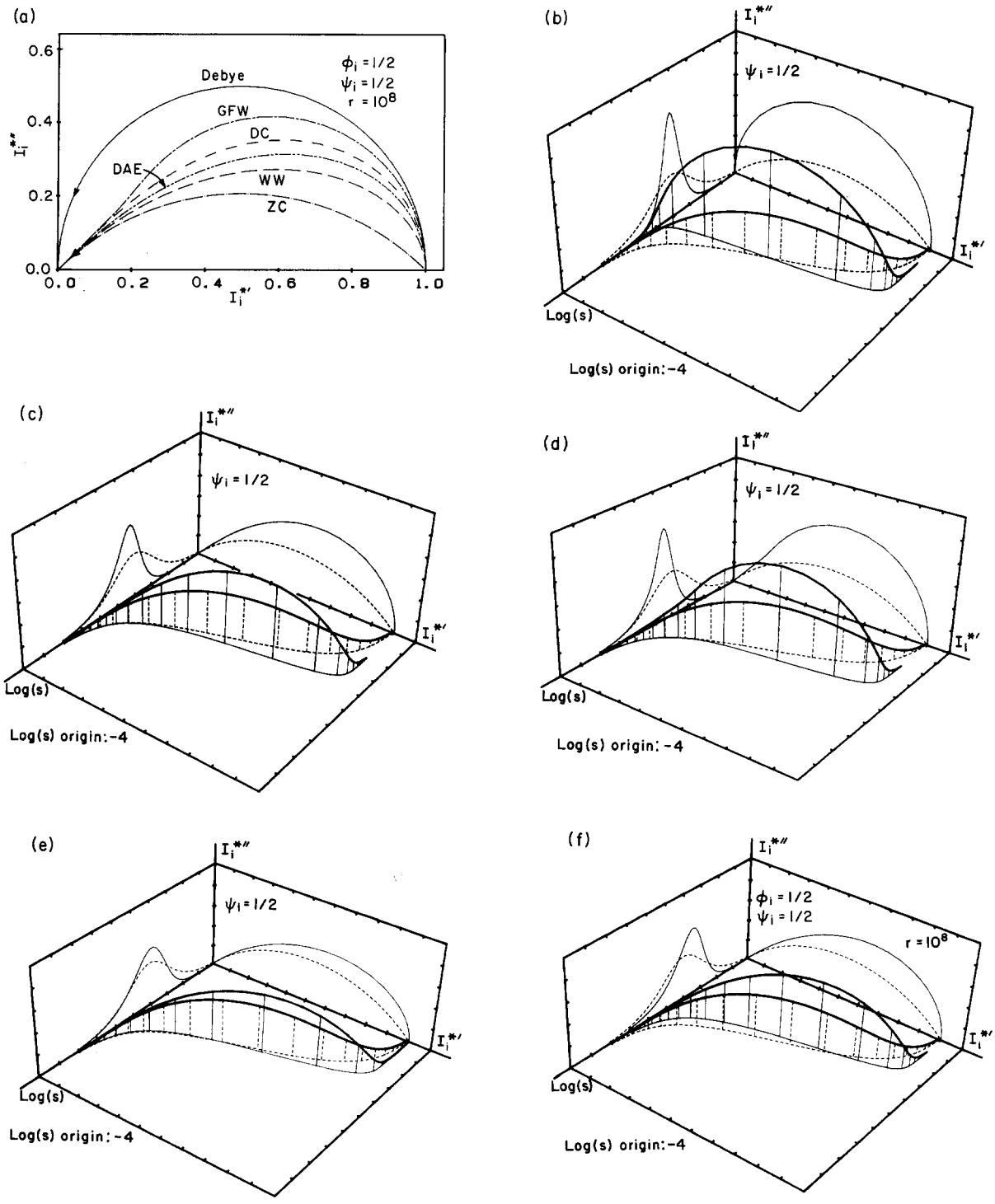

Fig. 3. Comparison of distributed elements with $\psi = \phi = 0.5$. (a) shows the I^* projections of the elements while the rest are 3-D perspective plots of the ZARC in comparison with the other response curves. For the 3-D curves, the log(s) units = 1 and the I units = 0.1. The responses plotted are (b) Debye, (c) DC, (d) GFW, (e) WW and (f) DAE_1.

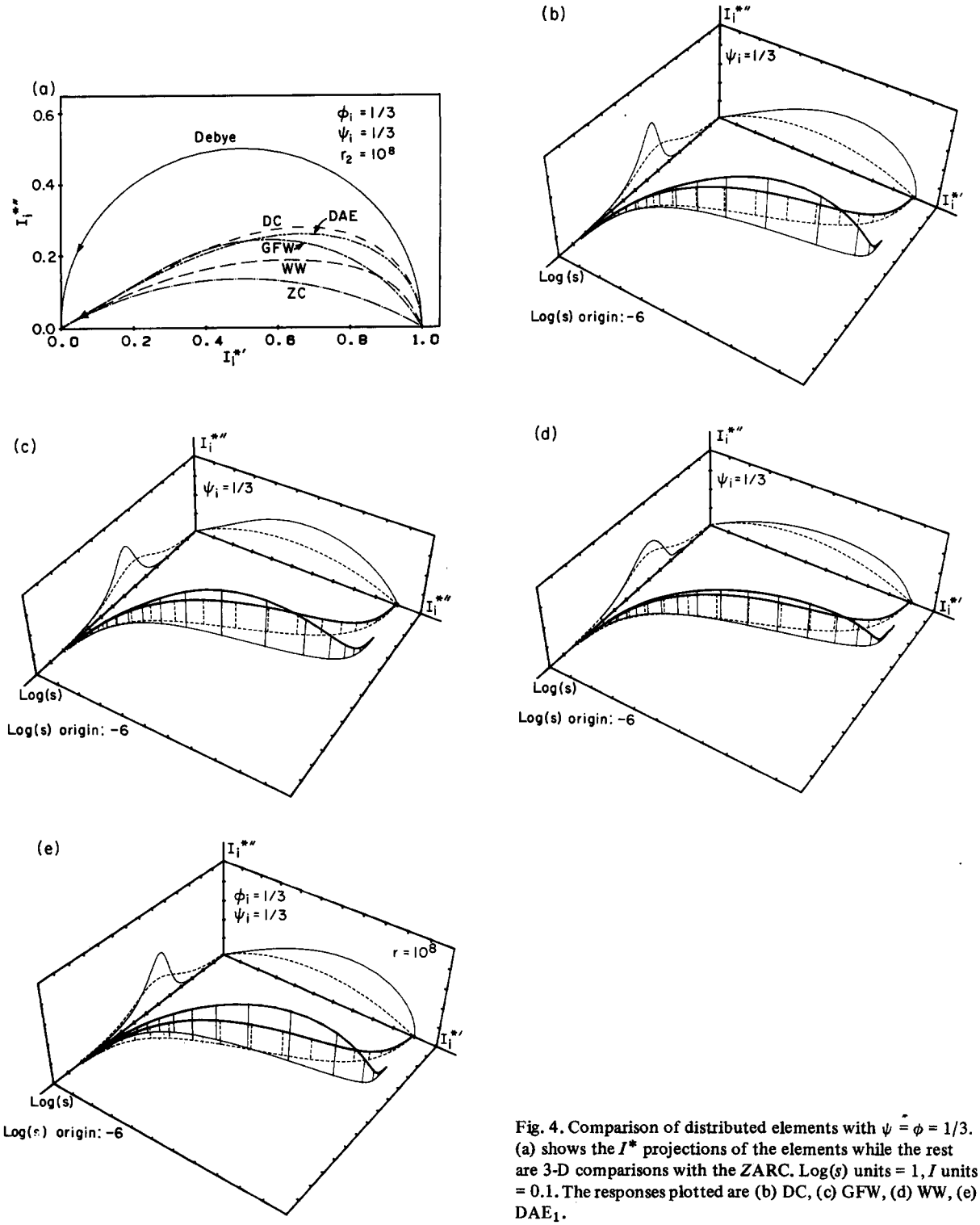

Fig. 4. Comparison of distributed elements with $\psi = \phi = 1/3$. (a) shows the I^* projections of the elements while the rest are 3-D comparisons with the ZARC. Log(s) units = 1, I units = 0.1. The responses plotted are (b) DC, (c) GFW, (d) WW, (e) DAE_1.

Fig. 3 presents a series of comparisons between the various elements at $\psi = 1/2$. Fig. 3a is a standard 2-D complex plane plot, provided to show in more detail what the complex plane projections of the 3-D perspective plots look like. For the 3-D plots of fig. 3b–3f each of the elements is presented on the same graph as a ZC element, chosen as a reference because of its high symmetry. In 3b a ZC is shown along with a standard Debye response. Note how much greater the frequency range of the ZC is over that of the Debye element – approximately 8 decades compared to 4 decades. The Debye also has a much sharper peak of I^* versus $\log(s)$, and it comes into the real axis vertically at either extreme of frequency as required by physical realizability.

The other elements are presented in figs. 3c through 3f. It is clear from the 2-D plot that all of the distributed elements have a CPE-like response at high frequencies, and all but the ZC have a Debye-like response at low frequencies (the DAE_1 also actually has a Debye-like response at high frequencies, but this will be treated in more depth later). It is no surprise that while the ZC is symmetric about the peak the other elements approach the peak more sharply from the low frequency side, acting more like the Debye curve from this end. The element with the sharpest peak is clearly the GFW (here, at $\psi = 1/2$, the same as a finite length Warburg or FLW). It also has a fairly distinct region of transition between Debye-like and CPE-like behavior. The DC and DAE have very similar shapes, an aspect which will be discussed later. The Williams–Watts curve appears closest to the ZARC with its fairly shallow peak, though it has been shown [23] actually to be closer to the asymmetric DC curve with some rescaling of parameters. Of all the elements in this figure, the WW is the one which is currently used most often in fitting data for dielectric systems, meaning that its I response is usually treated not as an impedance but as a complex dielectric constant.

Fig. 4 presents perspective plots of these same elements at $\psi = 1/3$ which bring out several interesting features. First, all of the elements have peaks which are spread out along a wider frequency range. The DC, GFW, and DAE_1 all exhibit a much longer region of CPE-like behavior at intermediate to high frequencies, while the WW and GFW curves no longer have much Debye-like behavior at low frequencies. Note also that the DAE_1 and DC are very similar in both the complex plane plot and in their full 3-D frequency response. For this exponent, the GFW does not have such a sharp region of transition between the peak and the region of CPE behavior.

To round off the study of the power-law-region behavior of these functions, fig. 5a gives a complex plane plot of the responses of all the distributed elements except the WW. For this exponent value of 2/3, the GFW more or less "blows up" in a large region where its projection is circular, with the center

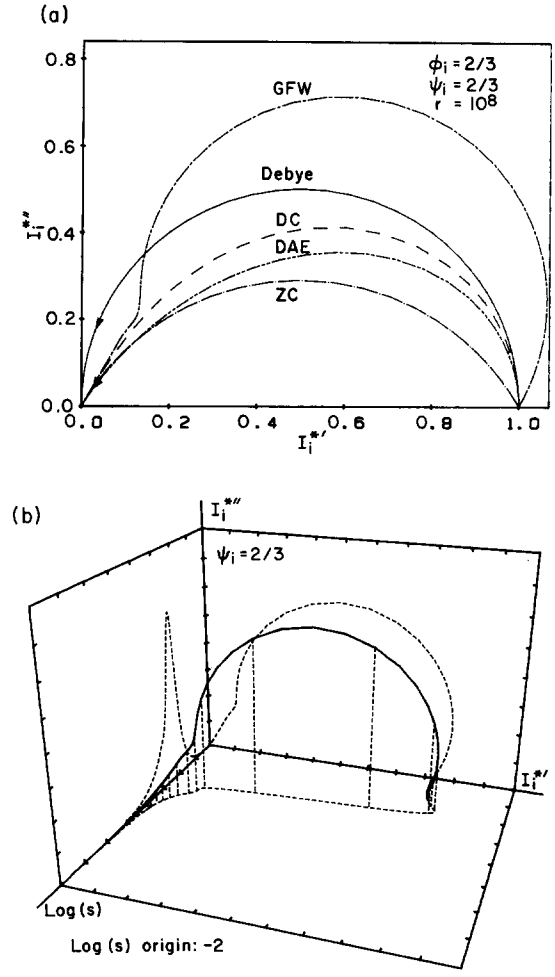

Fig. 5. Part (a) is a 2-D I^* plot of various distributed elements at $\psi = \phi = 2/3$ and (b) is a 3-D perspective plot of the GFW element displaying anomalous behavior at this value of ψ ($\log(s)$ unit = 1, I units = 0.1).

above the real axis. As fig. 5b shows, however, this behavior appears only over a narrow region of frequencies, thus exhibiting a very sharp peak in the $I^{*''}$-frequency plane. Because of this strange behavior, the GFW seems best used at values of ψ at or below 0.5. The behavior of the other elements clearly illustrates their approach to the Debye limit as $\psi \to 1$ for the DC and the ZC and for $\phi \gg 1$ for the DAE_1.

Because of the similarity between the DAE_1 and DC elements, several CNLS fits were made between the two elements to see how closely they corresponded. Reasonably close results were obtained for converged (upper limit $r \geqslant 10^8$) DAE_1 responses. In general, lower ψ and ϕ values gave better fits. Fits made using DAE data generated with smaller upper limits gave increasingly poor fits. The optimum exponent values for the DC were found to be lower than those for the DAE_1. Fig. 6 presents two of these fits

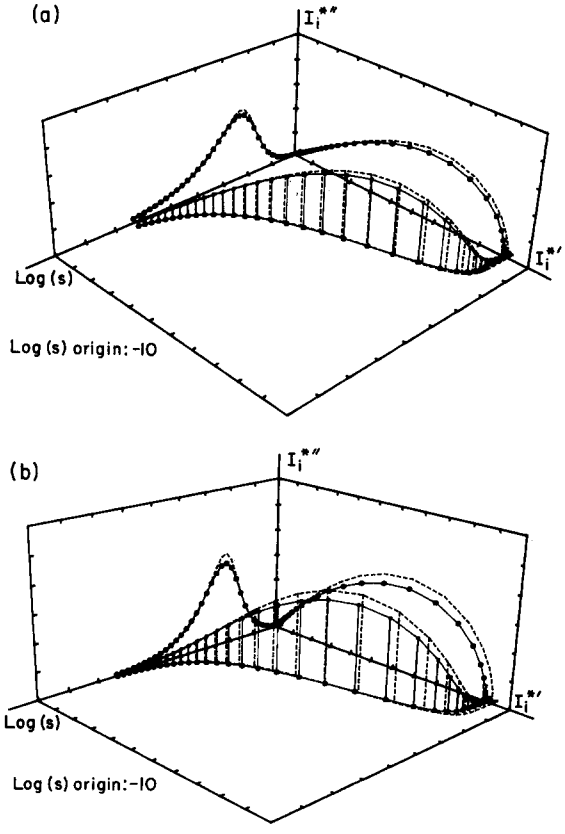

Fig. 6. Fits of Davidson–Cole model to the DAE_1 at (a) $\psi = \phi = 1/3$ and (b) $\psi = \phi = 1/2$. Log(s) unit = 1, I units = 0.1.

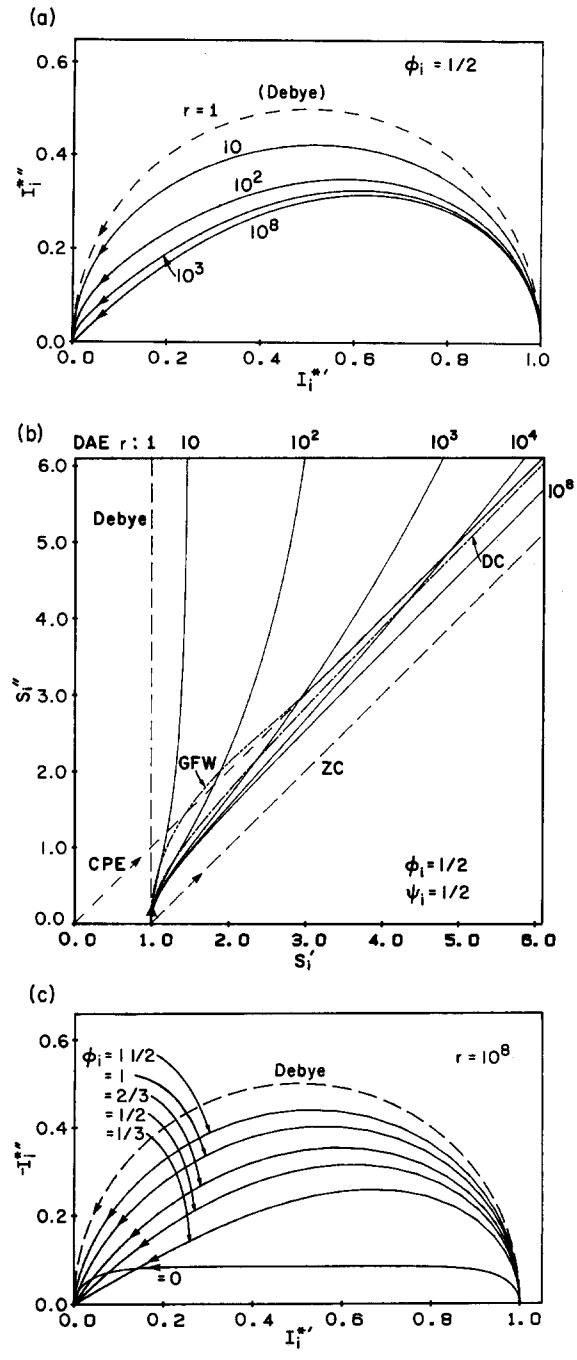

Fig. 7. DAE_1 properties. Part (a) shows the limiting r cases of the DAE_1 ranging from the Debye function to that of a converged DAE_1; (b) shows an S plot of the low frequency behavior of the DAE_1, with varying r values, in comparison with other distributed elements. Finally, (c) shows the ϕ variation of the DAE_1.

graphically, showing regions of difference. It is clear from these results that the DC has a significantly sharper peak than the DAE_1, though they are similar in other regions of the curve. Note that although the DAE_1 cannot fit the DC very accurately, it turns out, as already mentioned, that the more general DAE can do so [25].

There is a clear reason why the unconverged DAE_1 response, that with upper r limits on the order of 10^4 or less, would not fit the DC as well as that with $r \geqslant 10^8$. While at high frequencies the DC acts essentially like a CPE, the DAE eventually exhibits Debye-like behavior as $r \to 1$. The lower the upper limit is, the more dominant this behavior becomes. This is illustrated in figs. 7a and 7b. In the high frequency regions of the curves in 7a, it is possible to see the regions where the DAE_1 approaches the real axis almost vertically in all of the curves except the $r = 10^8$ one. Note also that the limit as $r \to 1$ is a Debye curve. Likewise, fig. 7b for the S function clearly shows how higher upper limits cause the DAE_1 to behave like a CPE over longer and longer regions. This graph also illustrates the limiting behavior of the other elements. Fig. 7c shows more completely the ϕ dependence of the DAE_1 for saturated r. The Debye limit is approached as $\phi \to \infty$. More details of general DAE response are given in ref. [7].

Acknowledgement

We much appreciate the support of the U.S. Army Research Office.

References

[1] J.R. Macdonald, J. Schoonman and A.P. Lehnen, J. Electroanal. Chem. 131 (1982) 77.
[2] Y.-T. Tsai and D.H. Whitmore, Solid State Ionics 7 (1982) 129.
[3] D.R. Franceschetti and J.R. Macdonald, J. Electroanal. Chem. 101 (1979) 307.
[4] A.K. Jonscher, Dielectric relaxation in solids (Chelsea Dielectrics Press, London, 1983).
[5] J.R. Macdonald, J. Schoonman and A.P. Lehnen, Solid State Ionics 5 (1981) 137.
[6] J.R. Macdonald and M.K. Brachman, Rev. Mod. Phys. 28 (1956) 393.
[7] J.R. Macdonald, J. Appl. Phys. 58 (1985) 1955; 58 (1985) 1971.
[8] E. Warburg, Wied. Ann. Phys. Chem. 67 (1899) 493.
[9] J.R. Macdonald, Phys. Rev. 92 (1953) 4.
[10] J. Llopis and F. Colom, in: Proc. 8th Meeting of the CITCE, Madrid, 1956 (Butterworths Sci. Publications, London) p. 414.
[11] D.R. Franceschetti and J.R. Macdonald, J. Electrochem. Soc. 129 (1982) 1754.
[12] H. Fricke, Philos. Mag. 14 (1932) 310.
[13] K.S. Cole and R.H. Cole, J. Chem. Phys. 9 (1941) 341.
[14] J.R. Macdonald, Solid State Ionics 13 (1984) 147.
[15] J. Schrama, Ph.D. Thesis (University of Leiden, The Netherlands) pp. 114–120.
[16] D.W. Davidson and R.H. Cole, J. Chem. Phys. 19 (1951) 1484.
[17] D. Ravaine and J.-L. Souquet, C.R. Acad. Sci. (Paris) 277C (1973) 489.
[18] J.R. Macdonald, Solid State Ionics 15 (1985) 159.
[19] J.R. Macdonald, J. Chem. Phys. 36 (1962) 345.
[20] R. Kohlrausch, Ann. Phys. (Leipzig) 12 (1847) 393.
[21] G. Williams and D.C. Watts, Trans. Faraday Soc. 66 (1970) 80.
[22] J.R. Macdonald, Phys. Rev. B, submitted.
[23] J.R. Macdonald and R.L. Hurt, J. Chem. Phys. 84 (1986) 496.
[24] J.R. Macdonald, J. Appl. Phys. 34 (1963) 538.
[25] J.R. Macdonald, work in progress.